Magnetism at high-index transition-metal surfaces and the effect of metalloid impurities: Ni(210)

W. T. Geng and A. J. Freeman
Department of Physics and Astronomy, Northwestern University, Evanston, Illinois 60208

R. Q. Wu
Department of Physics and Astronomy, California State University, Northridge, California 91330
(Received 29 June 2000; published 23 January 2001)

Structural, electronic, and magnetic properties near the Ni(210) surface and the effect of Li, B, P, and Ca impurities are determined by means of the all-electron total energy/atomic force full-potential linearized augmented plane wave method with the generalized gradient approximation. For the Ni(210) clean surface, simulated with an 11-layer slab, multilayer relaxation is found to be confined to the top three layers. The magnetic moment of the surface Ni layer, $0.79\mu_B$, is enhanced by 27%, compared with its bulk value. This result confirms the well-accepted understanding that the reduced coordination number at a clean transition-metal surface with a high index leads to enhanced magnetic moments. Boron and P strongly alter the atomic structure at the Ni(210) surface, whereas Li and Ca have only a slight influence, due to the weak chemical bonding with the nickel substrate. It is found that all four selected elements exert detrimental effects on the Ni(210) surface magnetism. The effects of B and P are stronger than those of Li and Ca, mainly due to their stronger hybridization with the nickel *d* states. An analysis of the results for B and P suggests that it is the stronger magnetization of its free standing monolayer that makes P more detrimental than B on the nickel surface magnetism.

DOI: 10.1103/PhysRevB.63.064427 PACS number(s): 75.70.Rf, 75.70.Cn, 71.15.Mb, 73.20.At

I. INTRODUCTION

During the last two decades, the electronic and magnetic properties of transition-metal (TM) surfaces has been a subject of great theoretical and experimental interest. The abrupt termination of the lattice leads to a variety of exotic phenomena such as magnetic moment enhancement and multilayer relaxation, which are now well recognized and generally explained in terms of the decrease in the coordination number and the increase in the localization of the *d* states near the surface.[1,2] Extensive studies have focused on low index surfaces, i.e., (001), (110), and (111). Little is known, however, whether this explanation holds true for surfaces with higher indices.

Nickel, a prototypical ferromagnetic transition metal, has received extensive investigations not only because of its intriguing electronic and magnetic properties, but also because of its technological importance as a catalyst, and its versatility in metallurgy and materials science. Ni(001) has been one of the most studied metal surfaces since the report of magnetically dead layers on this surface. Instead, first-principles investigations on 9-layer,[3] 5-layer,[4] and 7-layer[5] slabs have predicted a significant enhancement of the magnetic moment at this surface, which was later confirmed by experiment.[6] Full-potential linearized augmented plane wave[7] (FLAPW) studies on the (110)[8] and (111)[9] surfaces demonstrated similar enhancement, but to a smaller degree. Very recently, Mittendorfer *et al.*[10] studied comprehensively the structural, electronic, and magnetic properties of the low-index surfaces of ferromagnetic nickel with the first-principles pseudopotential method. Their results agree in general with the previous full-potential calculations and again indicated magnetism enhancement for these three surfaces. However, nickel surfaces with higher indicies remain unexplored.

On the other hand, the magnetism of the TM-TM interfaces[2,11] has been extensively studied and the effect of the chemisorption of gases on the surface magnetization of TM has also drawn more and more attention from both experimentalists and electronic structure theorists.[12] For the case of *sp* atomic overlayers adsorbed on a magnetic TM surface, the strong reduction of the surface magnetic moment or even magnetically dead layers and the induced magnetic moments at the adsorbate atoms are well-recognized experimentally.[13,14] However, many fundamental aspects of the interplay between adsorbate-TM bonding and TM magnetism remain unknown.

In this paper, we present results of an all-electron spin-polarized semirelativistic FLAPW study of the magnetism near the Ni(210) surface with and without an atomic overlayer, X (X=Li, B, P, or Ca). These elements, when segregated to the grain boundary in Ni, show significant strengthening or embrittling effect on the grain boundary cohesion.[15,16] A plausible thermodynamic model proposed by Rice and Wang[17] correlates the potency of a segregation impurity in reducing the ''Griffth work'' of a brittle boundary separation with the difference in binding energies for that impurity at the gran boundary and at the free surface. It is therefore of much interest to investigate the X-Ni bonding on the Ni surface. Exchange-correlation interactions between electrons are treated by the generalized gradient approximation (GGA), which is well-known to give a better description of the structural properties of $3d$ transition metals than does the local density approximation (LDA). For the Ni(210) clean surface, multilayer relaxation is found to be confined to the top three layers. Our calculations show that the surface magnetic moment of Ni(210) is $0.79\mu_B$, i.e., enhanced by 27% compared with the bulk value ($0.62\mu_B$) and even larger than that of the Ni(001) surface.[5] Thus, our first-principles result confirms, in the case of a magnetic transition metal surface with a high index, the well-accepted understanding

that the reduced coordination number and the resulting band narrowing at the surface lead to enhanced magnetic moments. B and P are found to introduce large relaxations of the atomic structure near the Ni(210) surface, whereas Li and Ca have only a slight influence. Interestingly, the strength of the perturbation largely scales with the binding energy of the overlayer. All these four *sp* elements exert detrimental effects on the magnetism of the Ni(210) surface, with the effects of B and P much more significant than those of Li and Ca. This is attributed to their stronger hybridization with the nickel *d* bands. Our first-principles results indicate that the strength of the detrimental effect varies roughly in scale with the *X*-Ni bonding strength. An analysis and comparison of B and P cases suggests that it is the stronger magnetization of its free-standing monolayer that makes P more detrimental than B on the nickel surface magnetism.

The rest of the paper is organized as follows: In Sec. II the calculational model and computational details are described. Results are presented in Sec. III, and finally, we give a summary in Sec. IV.

II. METHODOLOGY AND COMPUTATIONAL ASPECTS

The (210) free surface of fcc nickel is simulated by an 11-layer slab, and the adatoms, *X*, are placed pseudomorphically on the substitutional sites on both of its sides (cf. Fig. 1). The surface cell is chosen to be the primitive one, i.e., one atom in one layer. The two-dimensional (2D) lattice constants, 14.85 a.u. and 6.64 a.u., are taken from our GGA bulk calculations while the vertical nickel atom positions are determined by atomic force calculation. The open feature of this surface is very significant since the interatomic distance in the *x*-*y* plane is 6.64 a.u., while the vertical interlayer distance (unrelaxed) is only 1.484 a.u.

In the FLAPW method, no shape approximations are made to the charge densities, potentials, and matrix elements. Core states are treated fully relativistically and the valence states are treated semirelativistically (i.e., without spin-orbit coupling). The GGA formulas for the exchange-correlation potential are from Perdew *et al.*[18] An energy cutoff of 13 Ry was employed for the augmented plane-wave basis to describe the wave functions in the interstitial region, and a 140 Ry cutoff was used for the star functions depicting the charge density and potential. Summation over 49 *k* points in the irreducible 2D Brillouin zone is employed for *k*-space integrations.[19] Muffin-tin radii for nickel, Li, B, P, and Ca atoms were chosen as 2.0, 1.6, 1.3, 1.8, and 3.2 a.u., respectively. Within the muffin-tin spheres, lattice harmonics with angular momentum *l* up to 8 were adopted to expand the charge density, potential, and wave functions. Convergence is assumed when the average root-mean-square differences between the input and output charge and spin densities are less than 1×10^{-4} e/(a.u.)^3. The equilibrium atomic positions in the vertical direction were determined according to the calculated atomic forces being less than 0.004 Ry/a.u.. This tolerance results in an error to the atomic position of about 0.01 a.u., which results in a total energy error of about 0.001 Ry.

An inherent approximation in the slab model is its finite thickness. The choice of an appropriate thickness depends on the chemical or physical properties of interest and also on the specific system under investigation. The features of this model have been discussed at length for semiconductors by Appelbaum and Hamman.[20] It is known that for transition metals, a slab thickness of 20 a.u. is usually sufficient to obtain bulklike properties in the center of the slab and consequently true surface phenomena at the two slab/vacuum interfaces. Our interest here is the magnetism near the (210) surface of nickel, and hence, the criterion in judging whether an 11-layer slab is thick enough, is that the magnetic moments of the Ni atoms near the surface do not change when a thicker slab is used. In the study of the Ni(100) surface, Jepsen *et al.*[4] employed a 5-layer slab whereas Krakauer *et al.*[5] simulated it with a 7-layer slab. The use of the same thickness as theirs suggests a simulation of the Ni(210) surface with a 9- to 13-layer slab. Hence, in consideration of both obtaining reliable physics and managing the computing effort, we chose an 11-layer slab.

As a rigorous test to see whether such a slab is thick enough, we also carried out full FLAPW calculations on a

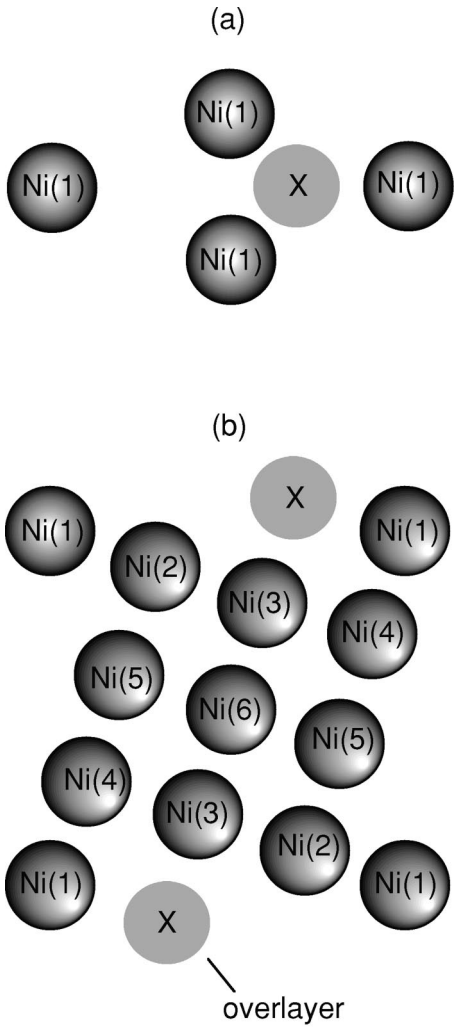

FIG. 1. Top view [panel *a*, plotted in (210) plane] and side view [panel *b*, plotted in (001) plane)] of the unit cell for the calculation of the Ni(210) surface.

TABLE I. The calculated interlayer distances (a.u.) near the clean Ni(210) surface by ferromagnetic (FM) and paramagnetic (PM) treatments.

	d_{12}	d_{23}	d_{34}	d_{45}	d_{56}	d_{67}
11-layer slab (FM)	1.32	1.47	1.58	1.47	1.51	
11-layer slab (PM)	1.31	1.48	1.57	1.47	1.51	
13-layer slab (FM)	1.31	1.48	1.58	1.48	1.51	1.48

13-layer slab for the clean Ni(210) surface. The calculated interlayer distances and magnetic moments in each muffin-tin sphere for these two slabs are listed in Table I and II, respectively. Although both the interlayer distances and the magnetic moments take the bulk values in the center of the 13-layer slab, good convergence is not found for either of them on going from the surface to the center of the slab. This is an indication that even the 13-layer slab is still not thick enough to give a highly realistic bulk environment for the center layer atoms. Nonetheless, a comparison of the two systems shows that for atoms near the surface, the first-principles calculations give very similar interlayer distances and magnetic moments. The discrepancy in interlayer distances is only 0.01 a.u., which is the same as the error in atomic positions. For the magnetic moments, the largest discrepancy happens for Ni(4). In the 11-layer slab, it is $0.65\mu_B$; in the 13-layer slab, it is $0.62\mu_B$. However, this difference (in percent) is still much smaller than that between the surface moment $0.79\mu_B$ and the bulk value $0.61\mu_B$ obtained from our FLAPW GGA calculation. It can thus be concluded that the 11-layer slab is an appropriate choice when the interest is in the physics of the first few layers near the Ni(210) surface.

III. CLEAN NI(210) SURFACE

A. Geometry

As stated above, the optimized atomic structure (cf. Table I) is obtained through atomic force calculations. To show the effect of spin polarization on the surface relaxation, we also performed spin unpolarized computations for this system.[21] The calculated interlayer distances are also listed in Table I. It is seen that the multilayer relaxation of Ni(210) occurs only in the top three layers, with Ni(3) and Ni(2) moving up and Ni(1) down. The surface layer relaxation, -12%, compares very well with that observed in the (110) case (-9%) by low-energy electron diffraction (LEED),[22] but is much larger than those found for the (001) surface (-3%) and the (111) surface ($<-2\%$),[22] which are more close packed. Unlike the case of the Fe(111) surface,[23] spin polarization has no noticeable effect on the Ni(210) surface relaxation. The differences between FM and PM cases are within 0.01 a.u. This can be explained by the fact that the magnetism of nickel is much weaker than that of iron.

B. Magnetism

The calculated magnetic moment in each muffin-tin sphere of the 11-layer slab (first row in Table II) shows a very large enhancement of the Ni(210) surface magnetism. The magnetic moment of the surface atoms $0.79\mu_B$ is 27% larger than the bulk value. For Ni(001), the surface magnetic moment is $0.70\mu_B$ from a 7-layer slab,[5] for which there was no structural optimization and LDA was used. To make a more meaningful comparison, we again studied Ni(001) in the present work. Here, the optimized GGA atomic structure was obtained by total energy/atomic force calculations. The magnetic moment of the Ni(001) surface atoms is $0.72\mu_B$, i.e., $0.07\mu_B$ smaller than that of Ni(210). The moment of the center layer is $0.61\mu_B$, which well recovers the bulk value. The large moment enhancement for Ni(210) can be explained by its more open structure. The (001) and (210) surfaces have a different coordination number and roughness ρ that is defined as the inverse of surface packing density calculated for a crystal made of touching hard spheres. For Ni(001), $\rho=1.273$; for Ni(210), $\rho=2.847$. The weaker in-plane Ni-Ni interaction gives the (210) surface a larger magnetism enhancement.

To gain a deeper insight into the surface induced charge rearrangement relevant for the surface magnetic moments, we now analyze the *l*-decomposed number of majority and minority valence electrons separately (cf. Table III). Similar to the Ni(001) case,[5] for the surface atoms the amount of majority *d*-like charge increases while the minority *d*-like charge decreases. Nevertheless, the total *d*-like charge is different for the surface and subsurface layers. The surface layer Ni(1) has more *d* electrons than the subsurface layers. The *s*- and *p*-like electrons in different layers scale very similarly for both the majority and minority spin electrons. As a result, the spin imbalance is larger for the surface atom than in the interior of the slab and the surface magnetism is enhanced compared with the interior.

TABLE II. The calculated magnetic moments (μ_B) in each muffin-tin sphere near the clean Ni(210) surface.

	Ni(1)	Ni(2)	Ni(3)	Ni(4)	Ni(5)	Ni(6)	Ni(7)
11-layer slab	0.79	0.70	0.65	0.65	0.65	0.69	
13-layer slab	0.78	0.71	0.64	0.62	0.67	0.66	0.61

TABLE III. Decomposition of the majority and minority valence charges in each muffin-tin sphere at the Ni(210) clean surface and in the bulk.

	s	*p*	*d*	Total
		Majority		
Ni(1)	0.13	0.06	4.35	4.54
Ni(2)	0.13	0.08	4.30	4.51
Ni(3)	0.13	0.10	4.26	4.50
Bulk	0.14	0.11	4.26	4.51
		Minority		
Ni(1)	0.13	0.06	3.57	3.76
Ni(2)	0.14	0.09	3.58	3.81
Ni(3)	0.14	0.11	3.61	3.86
Bulk	0.14	0.12	3.61	3.88

In order to examine the driving force of the charge rearrangement discussed above, we plotted the layer-projected density of states (DOS) of the surface layer Ni(1) (black lines) and an interior layer Ni(3) (gray lines) in Fig. 2. For both majority (panel *a*) and minority (panel *b*) states, Ni(1) has a smaller energy dispersion than Ni(3), indicating the well-known band-narrowing due to the lower atomic coordination at the surface. From Ni(3) to Ni(1), the minority DOS (panel *a*) experiences a significant increase at the Fermi energy. The increase of the number of unoccupied states is responsible for the loss of minority charge (cf. Table III). Panel (*c*) is a replot of panel (*b*) with a higher resolution. It is seen that above E_F, the spin-up DOS of Ni(1) is lower than that of Ni(3) and this decrease in the number of unoccupied states is responsible for the gain of majority charge (cf. Table III). With an increased majority charge and a decreased minority charge, the surface layer atoms have a larger magnetic moment than the interior atoms.

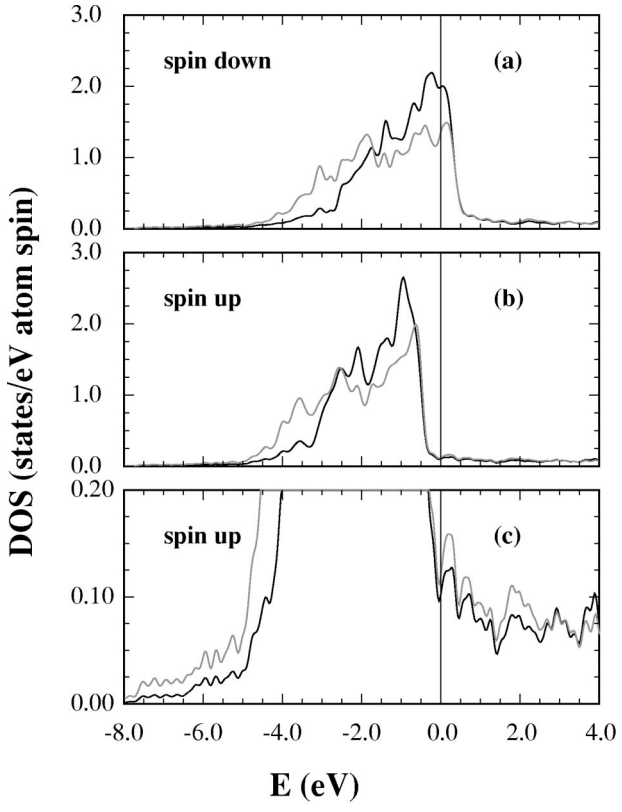

FIG. 2. Calculated layer-projected density of states (DOS) for Ni(1) (black lines) and Ni(3) (gray lines) in an 11-layer Ni(210) slab.

IV. NI(210) WITH A LI, B, P, OR CA OVERLAYER

A. Geometry

In order to understand the electronic and magnetic structures at the interface, we first examined the crystal structure. The calculated interlayer distances of each optimized X/Ni system are listed in Table IV; for comparison, the values for the clean surface are also listed. We can see that B and P introduce a much stronger perturbation to the Ni surface than do Li and Ca, as expected from their stronger chemical interaction with the nickel atoms. For instance, with the adsorption of P, d_{12} increases from 1.32 to 1.64 a.u. and d_{23} increases from 1.47 to 1.90 a.u. in the presence of B, whereas Li and Ca introduce only moderate relocation of the surface nickel atoms. A straightforward gauge of the multilayer relaxation is the sum of the absolute value of the change in each interlayer distance (denoted as ΔD) over the upper (lower) half of the slab relative to the clean surface; this appears to be the easiest way to take into account the effects on all the interlayer distances. Defined in this way, the perturbation strength ΔD is listed in Table IV. According to this definition, B and P have the same influence on the Ni(210) surface structure, which is much larger than that of Li and Ca. As mentioned above, this can be explained by the fact that B and P have stronger chemical bondings with Ni atoms than do Li and Ca. As a scale of the strength of chemical bonding, the binding energy ΔE_S of each overlayer (defined as the energy difference between the fully relaxed X/Ni system and the sum of energies of again fully relaxed clean Ni system and the free-standing X layer) is listed in Table IV. It is interesting to note that ΔD scales approximately to ΔE_S. Calcium, however, is an exception to this scaling behavior as it has a larger binding energy yet a smaller perturbation strength than Li. This is due to its extraordinarily large atomic size, and hence, large bond length with Ni, as seen from Table IV. With a Ca overlayer so high above, Ni(1), Ni(2), and Ni(3) have similar distances to Ca, and therefore, do not need to adjust themselves much (relative to their Ni neighbors) to form bonds.

We note that due to their strong chemical bonding with the surface Ni atoms, B and P can possibly form surface alloy on Ni(210) surface and can also possibly introduce faceting and reconstruction of this surface. That means the X/Ni(210) structure we obtained might not all be the most stable one. For instance, Kirby *et al.*[24] observed by LEED the adsorption of activated N can introduce (100) facets to the Ni(210) surface. However, a complete investigation of all the possible Ni(210) reconstruction and surface alloyings upon adsorption of X is apparently beyond the scope and effort of the present study. As our focus in this work is on

TABLE IV. Interlayer distances (a.u.) at the Ni(210) surface, with and without an X overlayer, and the perturbation strength and binding energy (defined in text) of the X overlayer on Ni(210).

Layer	Clean	Li/Ni	B/Ni	P/Ni	Ca/Ni
d_{X1}		2.24	0.02	0.64	2.72
d_{12}	1.32	1.19	1.34	1.64	1.36
d_{23}	1.47	1.58	1.90	1.67	1.47
d_{34}	1.58	1.60	1.40	1.47	1.55
d_{45}	1.47	1.45	1.52	1.50	1.46
d_{56}	1.51	1.51	1.49	1.49	1.51
$\Delta D(=\Sigma\lvert\Delta d\rvert)$		0.30	0.70	0.70	0.10
E_S(eV)		−2.28	−6.34	−5.99	−3.43

the chemical trend shown by different sp elements when adsorbed on this surface, we believe that the nonreconstruction treatment is a reasonable approximation.

B. Magnetism

The calculated magnetic moments in each muffin-tin sphere at the clean and X-adsorbed Ni(210) surface are listed in Table V. Following the idea of the definition of ΔD, we may employ a quantity Δm that is defined as the sum of the magnetic moment changes of nickel atoms over the upper (lower) half of the slab upon adsorption of the X overlayer, to describe quantitatively the effect of X on the surface magnetism of Ni. All four selected atomic sp overlayers are found to exert detrimental effects on the surface magnetism of Ni(210). In fact, B greatly reduces, and P kills almost completely, the magnetic moment of the top two surface layers Ni(1) and Ni(2). By comparison, Li and Ca introduce a moderate reduction. Furthermore, the effects of B and P are rather long ranged and affect the moment of the center layer, whereas the effects of Li and Ca are limited to their first rank neighbors, extending to Ni(3) and Ni(4), respectively.

The change of the magnetic moment inside the muffin-tin sphere of a Ni atom is associated with the relative change of the majority and minority charges in that sphere. This relative change has two possible origins: One is the interatom charge transfer; the other is the intra-atom charge transfer between majority and minority spins. At the Ni-X interface, the charge gain or loss of a nickel atom from its environment through Ni-X bonding has, in general, an unbalanced majority and minority spin distribution, and hence, a change in its magnetic moment. This interatom charge transfer originates from the ionic feature of the Ni-X chemical interaction. On the other hand, the covalent feature of the Ni-X interaction, i.e., Ni_d-X_{sp} hybridization, will broaden the distribution of the Ni electronic states. This change is mainly an electrostatically driven band-filling effect, in which the adsorption-induced loss of the majority states through Ni-X bonding is matched by an equal gain of the minority states. This intra-atom charge transfer, if any, will also alter the magnetic moment of this atom. The magnetization of the free-standing X monolayer, if existent, may exert an influence on the exchange splitting of the substrate, and hence an intra-atom charge transfer between majority and minority spins is made possible.

In Fig. 3, charge-density differences, obtained for each system by subtracting the superimposed charge density of a free standing X monolayer and the clean Ni reference slab (i.e., Ni positions are those after adsorption of X) from the charge density of the corresponding X/Ni system, are presented for B (panel a), P (panel b), Li (panel c), and Ca (panel d), respectively. In panel a and b, a significant charge accumulation can be found between X and Ni(3), indicating strong B-Ni(3) and P-Ni(3) chemical interactions. As a typical sp-d hybridization, the contours around Ni(3) exhibit a

TABLE V. The calculated magnetic moment $M(\mu_B)$ in each muffin-tin sphere at the Ni(210) surface, and that in the muffin-tin sphere of a free X monolayer. ΔM stands for the change in M upon adsorption of X. Δm is the summation of ΔM over the upper (lower) half of the slab.

Layer	Clean	Li/Ni	B/Ni	P/Ni	Ca/Ni
X (free)		0.00	0.43	1.54	0.00
X (on Ni)		−0.01	−0.01	−0.01	−0.05
Ni(1)	0.79	0.60	0.23	0.00	0.30
Ni(2)	0.70	0.60	0.09	0.01	0.48
Ni(3)	0.65	0.61	0.30	0.24	0.56
Ni(4)	0.65	0.65	0.59	0.51	0.55
Ni(5)	0.65	0.67	0.63	0.56	0.64
Ni(6)	0.69	0.68	0.61	0.60	0.69
$\Delta m(=\Sigma\Delta M)$		0.32	1.64	2.13	0.91

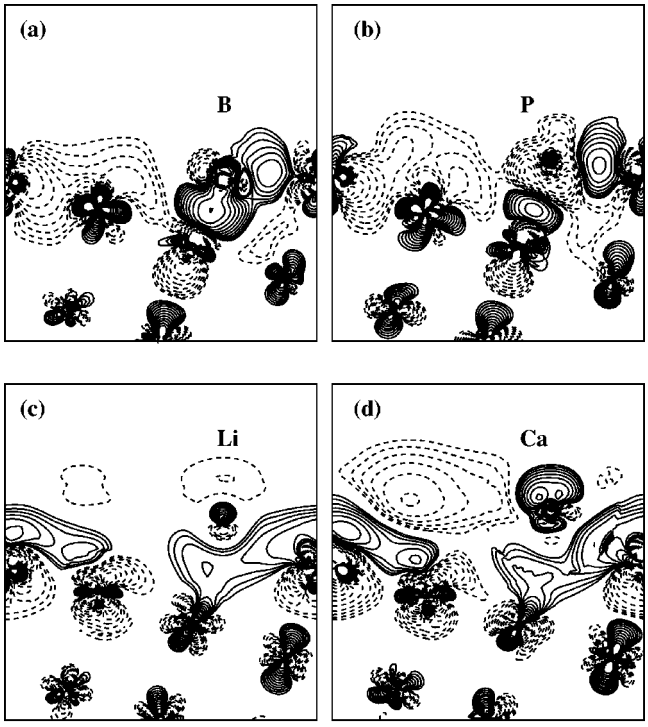

FIG. 3. Calculated total valence charge-density difference of the upper half of a 13-layer X/Ni(210) slab (X=B, P, Li, and Ca) in the (001) plane perpendicular to the surface. Contours start from 1×10^{-3} e/a.u.^{3} and increase successively by a factor of $\sqrt{2}$. Solid and dashed lines denote charge accumulation and depletion, respectively.

distorted d_{z^2} profile, while some electrons are removed from the inner region at the P site. The difference between the B-Ni(3) and the P-Ni(3) bond lies in the change of p_z state upon bonding. Unlike P-p_z, there is no loss of charge from B-p_z in the inner region at the B site. This difference is mainly due to the fact that B and P possess different numbers of p electrons.

For a free-standing B monolayer, the p_z state is empty since the p electrons occupy the p_x and p_y bonding states. In the B/Ni(210) system, the B p_z state lies lower in energy due to its hybridization with the d_{z^2} state of the underlying Ni(3) atom, and thus gains electrons from p_x and p_y states. B-Ni(1) and P-Ni(1) interactions are apparently weaker than B-Ni(3) and P-Ni(3) due to their large bond lengths and, as expected, show quite similar covalent bonding features. Charge accumulation is also found between X and Ni atoms in Li/Ni (panel c) and Ca/Ni (panel d) systems. Different from the B and P cases, Li-Ni and Ca-Ni interactions display a metallic nondirectionality bonding character. In the sense of interatom charge transfer, a metallic bond is basically a covalent bond, formed through band hybridization rather than charge transfer. Although stronger than Li-Ni bonding, the Ca-Ni interactions are hardly strong enough to be viewed as chemical bonds. This is because both Li's and Ca's s valence levels are significantly less tightly bound than the Ni d band; hence, there is only a relatively weak interaction between them.

The calculated changes in the total valence charges in the muffin-tin sphere of each Ni layer upon adsorption of an X overlayer are plotted in Fig. 4. Also plotted are changes in the magnetic moments, which can be easily obtained from the data in Table III. It is seen that all the Ni atoms gain more or fewer electrons upon adsorption of an atomic sp overlayer; the amounts are within 0.1 electron. Although B and P have a much stronger chemical interaction than do Li and Ca, the electrons gained by Ni atoms are not so different. This is because the interatom charge transfer is related mainly to the ionic, not covalent, feature of the X-Ni bonds. A comparison of their magnitudes indicates that the gain in total charge is only 10–20 % of the decrease of the Ni surface magnetic moment.

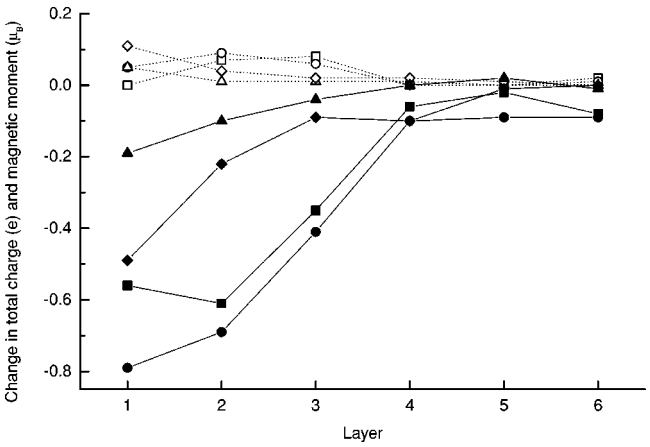

FIG. 4. The change in total valence charge in the muffin-tin sphere of each nickel atom, upon adsorption of a Li (open uptriangle), B (open square), P (open circle), and Ca (open diamond) monolayer; the change in spin magnetic moment in the muffin-tin sphere of each nickel atom, upon adsorption of a Li (solid uptriangle), B (solid square), P (solid circle), and Ca (solid diamond) monolayer.

As also revealed in many other cases of a magnetic transition metal overlayer grown on a nonmagnetic substrate, hybridization will frustrate the surrounding spin polarization.[2] In the present study of an atomic sp overlayer adsorbed on a magnetic transition metal surface, we found that for X=Li and Ca, the stronger the X_s-Ni$_d$ hybridization, the stronger detrimental effect of X on the magnetization of the Ni surface. In the cases of B and P, however, there is an extraordinary reduction of the magnetic moment of Ni(1) and Ni(2). The B(P)-Ni(3) interaction is stronger than B(P)-Ni(1) and B(P)-Ni(2), but the reduction of the magnetic moment of Ni(3) is smaller than that of Ni(1) and Ni(2). As discussed below, this appears to be related to the fact that both B and P free-standing monolayers are magnetic.

As isolated atoms, Li, Ca, B, and P possess a magnetic moment of 1.0, 0.0, 1.0, and 3.0μ_B, respectively. Although none of them shows magnetism in bulk, it is possible for an sp element to remain spin polarized in a free-standing monolayer, especially with the large lattice constant of the Ni(210) plane. Our first-principles calculations indicate that in such a monolayer, B and P have a magnetic moment inside the touching muffin-tin sphere of 0.43 and 1.54μ_B, respectively, whereas the ground state for Li and Ca is nonmagnetic. When adsorbed on Ni(210), however, both B and P lose

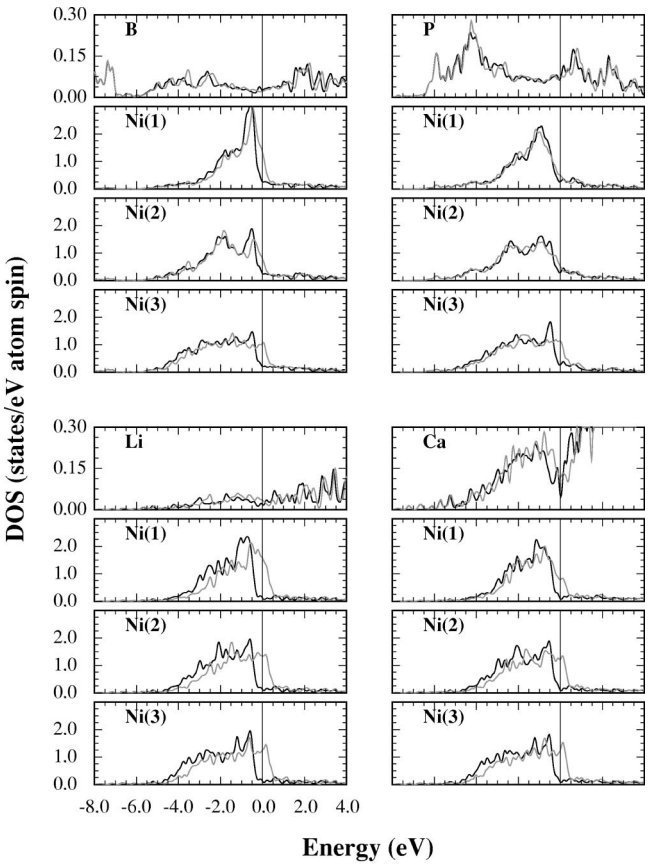

FIG. 5. Calculated layer-projected density of states (DOS) for X and the top three nickel layers in each X/Ni(210) 13-layer slab. Black lines and gray lines denote majority and minority states, respectively.

almost completely their spin polarization, carrying only a negligible moment of $-0.01\mu_B$ (cf. Table V) and coupling antiferromagnetically with the Ni substrate. Like the case of sulfur adsorbed on the Fe(001) surface,[25] the shift of the unoccupied B_p and P_p states from the minority to majority spectrum after adsorption indicates a stabilizing of the paramagnetic state of the atom.

To gain a more in-depth understanding of their poisoning effect, we now examine the electronic structure in energy space through the DOS. Figure 5 displays the layer-projected DOS for the majority and minority spins of X and the top three layers of the Ni substrate in each X/Ni(210) system. One remarkable feature shown is the similarity between the Li and Ca systems and that between the B and P systems, indicating their similarity in chemical interaction with Ni. Both B-Ni and P-Ni interactions show sp-d hybridization. Li-Ni and Ca-Ni interactions are rather weak. Although DOS peaks also appear on Li and Ca sites, they are mainly replica of Ni d states, i.e., tails of the Ni d states passively overlapping on the Li and Ca sites. Another important feature illustrated by Fig. 5 is the suppression of the minority states at E_F caused by the X_{sp}-Ni_d hybridization [cf. Fig. 2, for the clean Ni(210) surface]. Presumably, this suppression will give rise to the loss of the minority spin states and the gain of majority spin states, and thus diminish the Ni magnetic moment. Further, it is also clearly seen that B, P, and Ca cause decreases of the magnetic exchange splitting for the surface nickel layers. The effects of B and P are much larger than that of Ca, as can be understood by the fact that B-Ni and P-Ni bondings are much stronger than that of Ca-Ni. But with a lower bonding strength, the poisoning effect of P is more significant than that of B (cf. Fig. 4). It is thus suggestive that, aside from band hybridization, this difference in the poisoning effect should have other origin(s). One possibility is the difference in strength of the B-Ni and P-Ni exchange interaction.

Bearing this in mind, it is of interest to see what happens in a B(P)/Ni system when the B and P, as free-standing monolayers, have a zero magnetic moment. We found, by FLAPW calculations, that with the lattice constant of a Ni(001) plane, neither a B nor a P monolayer has a magnetic moment. We then investigated the poisoning effect of B and P overlayer on the magnetism at the Ni(001) surface simulated crudely by a three-layer slab. According to our calculations, when adsorbed on this Ni(001) three-layer film, the binding energy for the B and P monolayer is -3.59 and -2.56 eV, respectively. The poisoning effect Δm is $0.86\mu_B$ for B and $0.66\mu_B$ for P. Although a three-layer slab is by no means thick enough to well-describe free surface phenomena, the result is still quite illustrative. When nonmagnetic, the P monolayer has a smaller binding energy than B on the Ni(001) surface and exerts a weaker poisoning effect on the Ni magnetism than does B. Very likely, this conclusion will hold for a thicker Ni(001) film. We might then suggest that it is the large magnetic moment of the free monolayer that makes P more detrimental than B on the magnetism at the Ni(210) surface.

V. SUMMARY

We have performed first-principles studies of the atomic, electronic, and magnetic structures of a clean and X (X = Li, B, P, and Ca) adsorbed high-index magnetic transition metal surface—Ni(210). For the clean surface, the calculated magnetic moment of the surface layer atoms is $0.79\mu_B$, i.e., enhanced by 27% compared with the bulk value and is even larger than that of the (001) surface atoms ($0.72\mu_B$). This appears to confirm the well-accepted understanding that the reduced coordination number at clean metal surfaces leads to the enhanced magnetic moment in this case of a high-index surface. We found that all four selected sp elements exert a detrimental effect on the Ni(210) surface magnetism. The effects of B and P are much more significant than those of Li and Ca, mainly due to their stronger band hybridization with the Ni substrate. An analysis of the B and P cases suggests that it is the stronger magnetization of its free-standing monolayer that makes P more detrimental than B on the nickel surface magnetism.

ACKNOWLEDGMENTS

Work supported by a grant of Cray-J90 computer time at the DOD supported Arctic Region Supercomputing Center. Work at CSUN supported by the ONR (Grant No. N00014-95-1-0489).

[1] D. L. Adams, L. E. Petersen, and C. S. Sorensen, J. Phys. C **18**, 1753 (1985).
[2] A. J. Freeman and R. Wu, J. Magn. Magn. Mater. **100**, 497 (1991), and references therein.
[3] C. S. Wang and A. J. Freeman, Phys. Rev. B **21**, 4585 (1980).
[4] O. Jepsen, J. Madsen, and O. K. Andersen, J. Magn. Magn. Mater. **15-18**, 867 (1980); Phys. Rev. B **26**, 2790 (1982).
[5] H. Krakauer, A. J. Freeman, and E. Wimmer, Phys. Rev. B **28**, 610 (1983).
[6] R. Feder, S. F. Alvarado, E. Tamura, and E. Kisker, Surf. Sci. **127**, 83 (1983).
[7] E. Wimmer, H. Krakauer, M. Weinert, and A. J. Freeman, Phys. Rev. B **24**, 864 (1981), and references therein; M. Weinert, E. Wimmer, and A. J. Freeman, *ibid.* **26**, 4571 (1982).
[8] A. J. Freeman, C. L. Fu, and T. Oguchi, in *Computer Based Microscopic Description of the Structure and Properties of Materials*, edited by J. Broughton, W. Krakow, and S. T. Pantelides, Mater. Res. Soc. Symp. Proc. No. **63** (Materials Research Society, Pittsburgh, 1985), p. 1.
[9] C. L. Fu and A. J. Freeman, J. Phys. (Paris), Colloq. **49**, C8-1625 (1988).
[10] F. Mittendorfer, A. Eichler, and J. Hafner, Surf. Sci. **423**, 1 (1999).
[11] A. J. Freeman and C. L. Fu, in *Magnetic Properties of Low-Dimensional Systems*, edited by L. M. Falicov and J. L. Moran-Lopez (Springer, Berlin, 1986); R. Wu and A. J. Freeman, J. Magn. Magn. Mater. **200**, 498 (1999).
[12] S. Pick and H. Dreysse, Surf. Sci. **394**, 192 (1997).
[13] F. Passek and M. Donath, Phys. Rev. Lett. **71**, 2122 (1993).
[14] B. Sinkovic, P. D. Johnson, N. B. Brookes, A. Clarke, and N. V. Smith, Phys. Rev. B **52**, 6955 (1995).
[15] E. E. Brown and D. R. Muzyka, *Superalloys II* (Wiley, New York, 1987).
[16] R. E. Smith, W. T. Geng, C. B. Geller, R. Wu, and A. J. Freeman, Scr. Mater. **43**, 957 (2000).
[17] J. R. Rice and J. S. Wang, Mater. Sci. Eng., A **107**, 23 (1989).
[18] J. P. Perdew, K. Burke, and M. Ernzerhof, Phys. Rev. Lett. **77**, 3865 (1996).
[19] S. L. Cunningham, Phys. Rev. B **10**, 4988 (1974).
[20] J. A. Applebaum and D. R. Hamann, Rev. Mod. Phys. **48**, 479 (1976).
[21] According to our FLAPW GGA calculations, the paramagnetic fcc nickel has the same equilibrium lattice constant, i.e., 6.64 a.u., as the ferromagnetic case to an accuracy of 0.01 a.u.
[22] H. B. Michaelson, J. Appl. Phys. **48**, 4729 (1977); J. W. M. Frenken, R. G. Smeenk, and J. F. Van der Veen, Surf. Sci. **135**, 147 (1983); H. C. Lu, E. P. Gusev, E. Garfunkel, and T. Gustafsson, *ibid.* **352-354**, 21 (1996); D. L. Adams, L. E. Peterson, and C. S. Sorensen, J. Phys. C **18**, 1753 (1985).
[23] R. Wu and A. J. Freeman, Phys. Rev. B **47**, 3904 (1993).
[24] R. E. Kirby, C. S. Mckee, and L. V. Renny, Surf. Sci. **97**, 457 (1980).
[25] S. R. Chubb and W. E. Pickett, Phys. Rev. B **38**, 10 227 (1988).